An Implicit, Bidiagonal Numerical Method for Solving the Navier-Stokes Equations

E. von Lavante* and W. T. Thompkins Jr.†
Massachusetts Institute of Technology, Cambridge, Massachusetts

In recent years, much progress has been made in solving fluid dynamical problems using finite difference methods. Solving inviscid compressible problems in two and three dimensions has become almost routine with many suitable methods, explicit or implicit, available. The problem of compressible, viscous flows in complicated geometries remains, however, a major challenge. Here fine mesh spacing in the viscous flow regions makes the explicit methods with their simple boundary conditions extremely costly. Existing implicit methods can make use of large time steps, but require inversions of large block tridiagonal matrices. A method recently developed by MacCormack eliminates this disadvantage by introducing a predictor-corrector scheme requiring the inversion of only block bidiagonal matrices. It is the aim of present work to extend this method to allow solution of viscous, compressible problems in general coordinates for arbitrary two-dimensional geometries.

Introduction

IN recent years, much progress has been made in solving fluid dynamical problems using finite difference methods. Solving inviscid compressible problems in two and three dimensions has become almost routine with many suitable methods, explicit or implicit, available. The problem of compressible, viscous flow in complicated geometries remains, however, a major challenge.

Here fine mesh spacing in the viscous flow regions makes the explicit methods with their simple boundary conditions, such as the MacCormack scheme,[1,2] extremely costly. The existing implicit methods, such as Beam and Warming[3] or Pulliam and Steger,[4] make possible the use of large time steps, corresponding to Courant number of $\mathcal{O}(10^2)$, but require inversions of block tridiagonal matrices. A method recently developed by MacCormack[5] eliminates this disadvantage by introducing a predictor-corrector scheme requiring the inversion of only block bidiagonal matrices. The resulting difference equations are either upper or lower block bidiagonal equations that can be solved easily in one sweep. Unfortunately, this method was demonstrated only for the simple case of flat-plate shock/boundary-layer interaction. It is the aim of present work to expand this simple implicit method to allow solution of viscous, compressible problems in general coordinates for arbitrary two-dimensional geometries. A similar approach has been attempted by Kumar.[6]

The present method is very similar to the new MacCormack method. In the first step the explicit predictor-corrector finite difference method of Ref. 1 is used, approximating the governing fluid flow equations to second-order accuracy in space and time. Then the second step is used to remove the stability restriction of the first step by transforming the equations of the first step into an implicit form. The resulting matrices are block bidiagonal and can be easily solved. The Jacobian matrices of the governing flow equations are expressed in a convenient diagonalized form, making any matrix inversion unnecessary. The method was tested on a number of numerical examples, including incompressible and compressible Couette flow and a supersonic diffuser with shock/boundary-layer interaction.

Presented as Paper 82-0063 at the AIAA 20th Aerospace Sciences Meeting, Orlando, Calif., Jan. 11-14, 1982; submitted Jan. 25, 1982; revision received Sept. 26, 1982.

*Presently Assistant Professor, Aerospace Engineering Department, Texas A&M University.

†Associate Professor, Department of Aeronautics and Astronautics. Member AIAA.

Development of Algorithm

The two-dimensional compressible Navier-Stokes equations can be written in the conservation form

$$\frac{\partial U}{\partial t} + \frac{\partial F(U)}{\partial x} + \frac{\partial G(U)}{\partial y} = 0 \tag{1}$$

where

$$U = \begin{bmatrix} \rho \\ \rho u \\ \rho v \\ e_t \end{bmatrix} \qquad F = \begin{bmatrix} \rho u \\ \rho u^2 + \sigma_x \\ \rho u v + \tau_{xy} \\ (e_t + \sigma_x) u + \tau_{xy} v - k \dfrac{\partial T}{\partial x} \end{bmatrix}$$

$$G = \begin{bmatrix} \rho v \\ \rho u v + \tau_{xy} \\ \rho v^2 + \sigma_y \\ (e_t + \sigma_y) v + \tau_{xy} u - k \dfrac{\partial T}{\partial y} \end{bmatrix}$$

with

$$p = (\gamma - 1)\left[e_t - \tfrac{1}{2}\rho(u^2 + v^2)\right]$$

$$\sigma_x = p - \lambda\left(\frac{\partial u}{\partial x} + \frac{\partial v}{\partial y}\right) - 2\mu \frac{\partial u}{\partial x}$$

$$\tau_{xy} = -\mu\left(\frac{\partial u}{\partial y} + \frac{\partial v}{\partial x}\right)$$

$$\sigma_y = p - \lambda\left(\frac{\partial u}{\partial x} + \frac{\partial v}{\partial y}\right) - 2\mu \frac{\partial v}{\partial y}$$

Equation (1) can be expressed in nondimensional form by defining nondimensional variables

$$\rho' = \frac{\rho}{\rho_0}, \quad x' = \frac{x}{\ell_0}, \quad y' = \frac{y}{\ell_0}, \quad u' = \frac{u}{a_0}, \quad v' = \frac{v}{a_0}, \quad T' = \frac{T}{T_0}$$

$$p'=\frac{p}{\rho_0 a_0^2},\quad e_t'=\frac{e_t}{\rho_0 a_0^2},\quad \mu'=\frac{\mu}{\mu_0},\quad k'=\frac{k}{k_0},\quad t'=t\frac{a_0}{\ell_0}$$

$$Re_0=\frac{\rho_0 a_0 \ell_0}{\mu_0},\quad Pr_0=\frac{\mu_0 C_{p0}}{k_0}$$

The primes will be dropped later on for convenience. The vectors U, F, and G then become

$$U=\begin{bmatrix}\rho'\\ \rho' u'\\ \rho' v'\\ e_t'\end{bmatrix}$$

$$F=\begin{bmatrix}\rho' u'\\ \rho' u'^2+\sigma_x'\\ \rho' u' v'+\tau_{xy}'\\ (e_t'+\sigma_x')u'+\tau_{xy}'v'-k'\dfrac{1}{Pr_0 Re_0(\gamma-1)}\dfrac{\partial T'}{\partial x'}\end{bmatrix}$$

$$G=\begin{bmatrix}\rho' v'\\ \rho' u' v'+\tau_{xy}'\\ \rho' v'^2+\sigma_y'\\ (e_t'+\sigma_y')v'+\tau_{xy}'u'-k'\dfrac{1}{Pr_0 Re_0(\gamma-1)}\dfrac{\partial T'}{\partial y'}\end{bmatrix}$$

where

$$\sigma_x'=p'-\frac{\lambda'}{Re_0}\left(\frac{\partial u'}{\partial x'}+\frac{\partial v'}{\partial y'}\right)-2\frac{\mu'}{Re_0}\frac{\partial u'}{\partial x'}$$

$$\tau_{xy}'=-\frac{\mu'}{Re_0}\left(\frac{\partial u'}{\partial y'}+\frac{\partial v'}{\partial x'}\right)$$

$$\sigma_y'=p'-\frac{\lambda'}{Re_0}\left(\frac{\partial u'}{\partial x'}+\frac{\partial v'}{\partial y'}\right)-2\frac{\mu'}{Re_0}\frac{\partial v'}{\partial y'}$$

The equation of state for perfect gas becomes

$$p'=(\gamma-1)\left[e_t'-\tfrac{1}{2}\rho'(u'^2+v'^2)\right]$$

It is also interesting to note that

$$T'=\gamma p'/\rho;\qquad a'=\sqrt{T'};\qquad M=M'=u'/a'$$

In most of the practical cases it is necessary to transform the Cartesian coordinates x,y into some more general coordinates $\xi(x,y)$, $\eta(x,y)$. The strong conservation law form of Eq. (1) can be maintained as shown, for example, by Vinokur.[7] Equation (1) can then be written as

$$\frac{\partial \hat{U}}{\partial t}+\frac{\partial \hat{F}}{\partial \xi}+\frac{\partial \hat{G}}{\partial \eta}=0 \tag{2}$$

where

$$\hat{U}=U/J,\quad \hat{F}=(F\xi_x+G\xi_y)/J,$$
$$\hat{G}=(F\eta_x+G\eta_y)/J$$

J is the transformation Jacobian

$$J=\frac{1}{x_\xi y_\eta - x_\eta y_\xi}=\xi_x\eta_y-\xi_y\eta_x \tag{3}$$

The metrics ξ_x, ξ_y, etc., are easily formed using the relations

$$\xi_x=Jy_\eta \qquad \xi_y=-Jx_\eta$$
$$\eta_x=-Jy_\xi \qquad \eta_y=Jx_\xi \tag{4}$$

The method of numerical integration of Eq. (2) has been adopted from MacCormack,[5] where it is explained in detail. The resulting integration scheme will be therefore presented without detailed development. Equation (2) is integrated by the following implicit predictor-corrector set of finite difference equations:

Predictor

$$\Delta\hat{U}_{i,j}^n=-\Delta t\left(\frac{\Delta^+\hat{F}_{i,j}^n}{\Delta\xi}+\frac{\Delta^+\hat{G}_{i,j}^n}{\Delta\eta}\right)$$

$$\left(I-\Delta t\frac{\Delta^+|\hat{A}|^n}{\Delta\xi}\right)\left(I-\Delta t\frac{\Delta^+|\hat{B}|^n}{\Delta\eta}\right)\delta\overline{\hat{U}_{i,j}^{n+1}}=\Delta\hat{U}_{i,j}^n$$

$$\overline{\hat{U}_{i,j}^{n+1}}=\hat{U}_{i,j}^n+\delta\overline{\hat{U}_{i,j}^{n+1}}$$

Corrector

$$\Delta\overline{\hat{U}_{i,j}^{n+1}}=-\Delta t\left(\frac{\Delta^-\overline{\hat{F}^{n+1}}}{\Delta\xi}+\frac{\Delta^-\overline{\hat{G}^{n+1}}}{\Delta\eta}\right)$$

$$\left(I+\Delta t\frac{\Delta^-|\hat{A}|^{\overline{n+1}}}{\Delta\xi}\right)\left(I+\Delta t\frac{\Delta^-|\hat{B}|^{\overline{n+1}}}{\Delta\eta}\right)\delta\hat{U}_{i,j}^{n+1}=\overline{\hat{U}_{i,j}^{n+1}}$$

$$\hat{U}_{i,j}^{n+1}=\tfrac{1}{2}\left(\hat{U}_{i,j}^n+\overline{\hat{U}_{i,j}^{n+1}}+\delta\hat{U}_{i,j}^{n+1}\right) \tag{5}$$

where $|\hat{A}|$, $|\hat{B}|$ are matrices with positive eigenvalues, related to the Jacobians $\hat{A}=(\partial\hat{F}/\partial\hat{U})$ and $\hat{B}=(\partial\hat{G}/\partial\hat{U})$. $(\Delta^+/\Delta\xi)$ and $(\Delta^+/\Delta\eta)$ are one-sided forward differences, and $(\Delta^-/\Delta\xi)$ and $(\Delta^-/\Delta\eta)$ are one-sided backward differences.

The Jacobians $\hat{A}$ and $\hat{B}$ are related to the Jacobians $A=\partial F/\partial U$ and $B=\partial G/\partial U$ by

$$\hat{A}=A\xi_x+B\xi_y$$
$$\hat{B}=A\eta_x+B\eta_y \tag{6}$$

and are given in, for example, Steger[8]

$$\hat{A}=\begin{bmatrix}0 & \xi_x & \xi_y & 0\\ -uU_\xi+\xi_x\beta\alpha & U_\xi-(\beta-1)\xi_x u & \xi_y u-\beta\xi_x v & \beta\xi_x\\ vU_\xi+\xi_y\beta\alpha & -\beta\xi_y u+\xi_x v & U_\xi-(\beta-1)\xi_y v & \beta\xi_y\\ U_\xi\left[\alpha(\beta-1)-\dfrac{a^2}{\beta}\right] & -\beta U_\xi u+\left(\dfrac{a^2}{\beta}+\alpha\right)\xi_x & -\beta U_\xi v+\left(\dfrac{a^2}{\beta}+\alpha\right)\xi_y & (\beta+1)U_\xi\end{bmatrix} \tag{7}$$

Here $\alpha = \frac{1}{2}(u^2+v^2)$, $\beta = (\gamma-1)$, $a = \sqrt{\gamma(p/\rho)}$, and U_ξ, U_η are the contravariant velocities

$$U_\xi = u\xi_x + v\xi_y$$

$$U_\eta = u\eta_x + v\eta_y$$

The Jacobian matrix B is obtained by substituting U_ξ, ξ_x, ξ_y by U_η, η_x, η_y.

The integration scheme of Eq. (5) can be much simplified by diagonalizing $\hat{A}$ and $\hat{B}$. Once the eigenvalues of $\hat{A}$ and $\hat{B}$ are known, it is possible to express $\hat{A}$ and $\hat{B}$ in the form

$$\hat{A} = \hat{S}_\xi^{-1}\Lambda_A\hat{S}_\xi$$

$$\hat{B} = \hat{S}_\eta^{-1}\Lambda_B\hat{S}_\eta \tag{8}$$

where Λ_A and Λ_B are diagonal matrices consisting of the eigenvalues of $\hat{A}$, $\Lambda_{A,1},\ldots,\Lambda_{A,4}$, and $\hat{B}$, $\Lambda_{B,1},\ldots\Lambda_{B,4}$, respectively. The matrices $\hat{S}_\xi$ and $\hat{S}_\eta$ are constructed using the eigenvectors of $\hat{A}$ and $\hat{B}$, respectively, as columns. It should be noted that this factorization is not unique and the matrix elements depend on the similarity transform to find the eigenvalues of $\hat{A}$ and $\hat{B}$.

Warming et al.[9] found the eigenvalues and eigenvectors of the nonconservative system corresponding to Eq. (1)

$$\frac{\partial\tilde{U}}{\partial t} + \tilde{A}\frac{\partial\tilde{U}}{\partial x} + \tilde{B}\frac{\partial\tilde{U}}{\partial y} = 0$$

They give the eigenvector matrix T such that if $\tilde{P} = k_1\tilde{A} + k_2\tilde{B}$, then

$$T^{-1}\tilde{P}T = \begin{bmatrix} \lambda_1 & & & 0 \\ & \lambda_2 & & \\ 0 & & \lambda_3 & \\ & & & \lambda_4 \end{bmatrix} = \Lambda$$

for arbitrary k_1, k_2. The matrix T is

$$T = \begin{bmatrix} 1 & 0 & \rho/\sqrt{2}a & \rho/\sqrt{2}a \\ 0 & K_2 & K_1/\sqrt{2} & -K_1/\sqrt{2} \\ 0 & -K_1 & K_2/\sqrt{2} & -K_2/\sqrt{2} \\ 0 & 0 & \rho a/\sqrt{2} & \rho a/\sqrt{2} \end{bmatrix} \quad \begin{matrix} K_1 = k_1/\sqrt{k_1^2+k_2^2} \\ K_2 = k_2/\sqrt{k_1^2+k_2^2} \end{matrix}$$

The Jacobians A and B of the conservative system [Eq. (1)] are obtained from the nonconservative $\tilde{A}$ and $\tilde{B}$ by

$$\tilde{A} = M^{-1}AM \qquad \tilde{B} = M^{-1}BM \tag{9}$$

where

$$M = \begin{bmatrix} 1 & 0 & 0 & 0 \\ u & \rho & 0 & 0 \\ v & 0 & \rho & 0 \\ \alpha & \rho u & \rho v & \dfrac{1}{\beta} \end{bmatrix}$$

If now $P = k_1A + k_2B$ for the conservative system then $\tilde{P} = M^{-1}PM$ gives the proper relation for conversion of P from conservative to nonconservative. Both P and $\tilde{P}$ have the same eigenvalues, so that

$$P = MT\Lambda(MT)^{-1} \tag{10}$$

Equation (10) can be used to find the matrices $\hat{S}_\xi$, Λ_A, $\hat{S}_\xi^{-1}$ and $\hat{S}_\eta$, Λ_B, $\hat{S}_\eta^{-1}$ in Eq. (8). One can, for example, set the arbitrary k_1 and k_2 to $k_1 = \xi_x$, $k_2 = \xi_y$ and obtain

$$P = \xi_xA + \xi_yB = \hat{A}$$

The comparison of Eqs. (10) and (8) leads to

$$\hat{S}_\xi = MT \tag{11}$$

It is easy to find $\hat{S}_\xi$ by carrying out the multiplication in Eq. (11). The result is

$$\hat{S}_\xi^{-1} = \begin{bmatrix} 1 & 0 & \rho/a\sqrt{2} & \rho/a\sqrt{2} \\ u & \rho\xi_y/c_1 & \rho\left(\dfrac{u}{a} + \dfrac{\xi_x}{c_1}\right)\Big/\sqrt{2} & \rho\left(\dfrac{u}{a} - \dfrac{\xi_x}{c_1}\right)\Big/\sqrt{2} \\ v & -\rho\xi_x/c_1 & \rho\left(\dfrac{v}{a} + \dfrac{\xi_y}{c_1}\right)\Big/\sqrt{2} & \rho\left(\dfrac{v}{a} - \dfrac{\xi_y}{c_1}\right)\Big/\sqrt{2} \\ \alpha & \rho(u\xi_y - v\xi_x)/c_1 & \rho\left(\dfrac{\alpha}{a} + \dfrac{U_\xi}{c_1} + \dfrac{a}{\beta}\right)\Big/\sqrt{2} & \rho\left(\dfrac{\alpha}{a} - \dfrac{U_\xi}{c_1} + \dfrac{a}{\beta}\right)\Big/\sqrt{2} \end{bmatrix} \tag{12}$$

where $c_1 = \sqrt{\xi_x^2 + \xi_y^2}$. $\hat{S}_\xi^{-1}$ is found simply from $\hat{S}_\xi^{-1} = T^{-1}M_\xi^{-1}$

$$\hat{S}_\xi = \begin{bmatrix} 1 - \dfrac{\alpha\beta}{a^2} & \beta u/a^2 & \beta v/a^2 & -\beta/a^2 \\ (-u\xi_y + v\xi_x)/\rho c_1 & \xi_y/\rho c_1 & -\xi_x/\rho c_1 & 0 \\ \left(\dfrac{\alpha\beta}{a} - \dfrac{U_\xi}{c_1}\right)\Big/\rho\sqrt{2} & \left(\dfrac{\xi_x}{c_1} - \dfrac{\beta u}{a}\right)\Big/\rho\sqrt{2} & \left(\dfrac{\xi_y}{c_1} - \dfrac{\beta v}{a}\right)\Big/\rho\sqrt{2} & \beta/\rho a\sqrt{2} \\ \left(\dfrac{\alpha\beta}{a} + \dfrac{U_\xi}{c_1}\right)\Big/\rho\sqrt{2} & -\left(\dfrac{\xi_x}{c_1} + \dfrac{\beta u}{a}\right)\Big/\rho\sqrt{2} & -\left(\dfrac{\xi_y}{c_1} + \dfrac{\beta v}{a}\right)\Big/\rho\sqrt{2} & \beta/\rho a\sqrt{2} \end{bmatrix} \tag{13}$$

And finally Λ_A is formed from eigenvalues of $\hat{A}$. These are given by, for example, Steger[8]

$$\Lambda_A = \begin{bmatrix} U_\xi & 0 & 0 & 0 \\ 0 & U_\xi & 0 & 0 \\ 0 & 0 & U_\xi + ac_1 & 0 \\ 0 & 0 & 0 & U_\xi - ac_1 \end{bmatrix} \tag{14}$$

$\hat{S}_\eta$, Λ_B, and $\hat{S}_\eta^{-1}$ are similar; they can be found by replacing ξ_x, ξ_y, and U_ξ by η_x, η_y, and U_η. Following closely the MacCormack approach in Ref. 5, the matrices $|\hat{A}|$ and $|\hat{B}|$ in Eq. (5) are formed by replacing the matrices Λ_A and Λ_B by positively valued diagonal matrices D_A and D_B such that

$$D_A = |\Lambda_A| + \lambda_A I \qquad D_B = |\Lambda_B| + \lambda_B I \tag{15}$$

where

$$\lambda_A = \frac{2\nu}{\rho\Delta\xi}(\xi_x^2+\xi_y^2) - \frac{1}{2}\frac{\Delta\xi}{\Delta t}$$

$$\lambda_B = \frac{2\nu}{\rho\Delta\eta}(\eta_x^2+\eta_y^2) - \frac{1}{2}\frac{\Delta\eta}{\Delta t}$$

and

$$\nu = \max\left(\frac{\mu}{Re_0}, \frac{(\lambda+2\mu)}{Re_0}, \frac{k\gamma}{Pr_0 Re_0}\right)$$

Equation (15) for D_A and D_B assumes that viscous effects are modeled in the implicit part of the scheme by addition of the terms λ_A, λ_B which include viscosity through the coefficient ν. The elements of D_A, D_B are non-negative; negative values of the elements of D_A, D_B mean that the CFL condition is met and there is no need to use the implicit portion of Eq. (5). The integration scheme [Eq. (5)] can now be carried out in the following steps:

1) Let

$$\Delta\hat{U}_{i,j}^n = -\Delta t\left(\frac{\Delta^+\hat{F}_{i,j}^n}{\Delta\xi} + \frac{\Delta^+\hat{G}_{i,j}^n}{\Delta\eta}\right)$$

at every point inside the calculational domain.

2) Solve

$$\left(I - \Delta t\frac{\Delta^+|\hat{A}|^n}{\Delta\xi}\right)\left(I - \Delta t\frac{\Delta^+|\hat{B}|}{\Delta\eta}\right)\delta\overline{\hat{U}_{i,j}^{n+1}} = \Delta\hat{U}_{i,j}^n \quad \text{for} \quad \delta\overline{\hat{U}_{i,j}^{n+1}}$$

This is done in two steps by denoting

$$\delta\hat{U}_{i,j}^* = \left(I - \Delta t\frac{\Delta^+|\hat{B}|}{\Delta\eta}\right)\delta\overline{\hat{U}_{i,j}^{n+1}}$$

resulting in two vector equations:

a) $$\left(I - \Delta t\frac{\Delta^+|\hat{A}|^n}{\Delta\xi}\right)\delta\hat{U}_{i,j}^* = \Delta\hat{U}_{i,j}^n$$

b) $$\left(I - \Delta t\frac{\Delta^+|\hat{B}|^n}{\Delta\eta}\right)\delta\overline{\hat{U}_{i,j}^{n+1}} = \delta\hat{U}_{i,j}^*$$

A closer look at step 2a reveals that it is an upper bidiagonal equation that can be solved by sweeping in decreasing ξ direction for a constant η. Substituting Eq. (8) in step 2a and some simple manipulation leads to

$$(I + \Delta t\hat{S}_{\xi_{i,j}}^{-1} D_{A_{i,j}} \hat{S}_{\xi_{i,j}})\delta\hat{U}_{i,j}^* = \Delta\hat{U}_{i,j}^n + \Delta t|\hat{A}|_{i+1,j}\delta\hat{U}_{i+1,j}^* \tag{16}$$

Denoting $w = \Delta\hat{U}_{i,j}^n + \Delta t|\hat{A}|_{i+1,j}\delta\hat{U}_{i+1,j}^*$ and some matrix multiplication gives finally

$$\delta\hat{U}_{i,j}^* = \hat{S}_\xi^{-1}(I + \Delta t D_A)^{-1} S_\xi w \tag{17}$$

Equation (17) can be very easily solved since $\hat{S}_\xi$ and $\hat{S}_\xi^{-1}$ are known and the inversion of the diagonal matrix $(I+\Delta t D_A)$ is trivial. After all $\delta U_{i,j}^*$ inside the calculational domain are determined, step 2b can be carried out in the same manner. The corrector steps are analogous to the predictor steps. The major problem in the scheme described above is finding the proper boundary values of the expression $\Delta t|\hat{B}|_{i,j}\delta\hat{U}_{i,j}$ for $i=i_{max}$, $i=1$ and $j=j_{max}$ and $j=1$, because these are not known at the time when the sweep begins.

Boundary Conditions

Since the present method uses upwind spatial derivatives, a starting value of the expression $\Delta t|\hat{B}|\delta\hat{U}$ or $\Delta t|\hat{A}|\Delta\hat{U}$ is needed for both the predictor and corrector. For simplicity, we will denote these expressions δW; they represent the implicit part of the boundary conditions. The explicit boundary conditions, needed for evaluation of the expression ΔU^n, are obtainable more easily. At the boundary, Eq. (16) will take the following form:

$$(I + \Delta t\hat{S}_{\xi_{i,j}}^{-1} D_{A_{i,j}} \hat{S}_{\xi_{i,j}})\delta\hat{U}_{i,j}^* = \Delta\hat{U}_{i,j}^n + \delta w \tag{18}$$

In order to maintain the unconditional stability of Eq. (5), the value of δW would have to be evaluated implicitly. An improper treatment of the implicit part of the boundary conditions, such as lagging in time, will limit the stability region of Eq. (5) to CFL members of $\mathcal{O}(1)$. The present work developed some ad hoc procedures for determining the value of δw that gave satisfactory results for the test cases used. A more vigorous treatment of the boundary conditions for the present method will be required to develop their generally valid formulation.

The following boundary conditions were implemented:

1) Supersonic inflow boundary. At these boundaries, all the eigenvalues of A are positive, so that all characteristics point from outside into the computational domain. All the elements of U are therefore specified at this boundary. For time-independent boundary conditions one obtains: ρ, ρu, ρv, e = const; $\delta W = 0$.

2) Supersonic outflow boundary. Here all the characteristics have the direction from inside to outside. All the values of U must be therefore extrapolated from the computational domain. The explicit part of the boundary conditions does not represent any problems; the elements of U are in this case linearly extrapolated from the computational domain

$$\hat{U}_{i_{max}} = 2\hat{U}_{i_{max}-1} - \hat{U}_{i_{max}-2} \tag{19}$$

The same extrapolation was applied to δw.

$$\delta w = 2(|\hat{A}|\delta\hat{U})_{i_{max}-1} - (|\hat{A}|\delta\hat{U})_{i_{max}-2} \tag{20}$$

Since, at the time of evaluation of δW, the expressions on the left-hand side of Eq. (20) are not known, δW would have to be calculated by using an implicit scheme at the three points i_{max}, i_{max-1}, and i_{max-2}.

In the present work the CFL number in the x direction was always less than 1, so that purely explicit boundary conditions were used, giving Eq. (19) and $\delta w = 0$.

3) Solid-wall boundary. The wall was placed between the first and second grid point and reflective boundary conditions

were used. The explicit boundary conditions for an adiabatic wall are then

$$\rho u_{i,1} = -\rho u_{i,2}; \quad \rho v_{i,1} = -\rho v_{i,2}$$

$$\rho_{i,1} = \rho_{i,2}; \quad e_{i,1} = e_{i,2}$$

The corrector value of δw can be obtained using the same principle from the predictor value of $\Delta t\,|B|\delta\hat{U}$ at the point $j=2$

$$\delta W^{n+1} = R \cdot \Delta t(\,|\hat{B}|\delta\hat{U})^{\overline{n+1}}_{j=2} \tag{21}$$

where

$$R = \begin{bmatrix} 1 & 0 & 0 & 0 \\ 0 & -1 & 0 & 0 \\ 0 & 0 & -1 & 0 \\ 0 & 0 & 0 & 1 \end{bmatrix}$$

There still remains the problem of finding the predictor value of δw. The present work used the following procedure:

$$\delta w^{\overline{n+1}} = R \cdot \Delta t(\,|B|\delta\hat{U})^{n}{}_{j=2} = \delta w^n$$

while switching the direction of the predictor sweep after every completed predictor-corrector sequence. This is equivalent to lagging the boundary value of change of flux one-half time step. The solid walls may also be placed at the first grid node and the condition $\delta W = 0$ used.

4) Periodic boundaries. The periodic boundaries were again placed between the first and second grid point, and δW was lagged one-half step. Placing the periodic boundaries at, for example, $i = 1 + (½)$ and $i = i_{\max} - (½)$ resulted in the following scheme: for the predictor sweeping in the direction of increasing i,

$$\rho^{\overline{n+1}}_{1,j} = \rho^n_{i_{\max}-1,j}; \quad u^{\overline{n+1}}_{1,j} = u^n_{i_{\max}-1,j}; \quad v^{\overline{n+1}}_{1,j} = v^n_{i_{\max}-1,j};$$

$$e^{\overline{n+1}}_{1,j} = e^n_{i_{\max}-1,j}; \quad \delta w^{\overline{n+1}}_{1,j} = \delta w^n_{i_{\max}-1,j}$$

and for the corrector,

$$\rho^{n+1}_{i_{\max},j} = \rho^{\overline{n+1}}_{2,j}, \quad u^{n+1}_{i_{\max},j} = u^{\overline{n+1}}_{2,j}, \quad v^{n+1}_{i_{\max},j} = v^{\overline{n+1}}_{2,j}$$

$$e^{n+1}_{i_{\max},j} = e^{\overline{n+1}}_{2,j}, \quad \delta w^{n+1}_{i_{\max},j} = \delta w^{\overline{n+1}}_{2,j}$$

Here, the grid lines are assumed to be orthogonal at these boundaries.

No attempt was made at this time to create nonreflective implicit boundary conditions based on the characteristics of Eq. (5). Note also that the outflow boundary conditions are only explicit. The present method is therefore limited to supersonic inflow and supersonic outflow boundaries with CFL number $\mathcal{O}(1)$ in the outflow direction or periodic inflow/outflow.

Examples

The present numerical method was tested on two examples, the Couette flow and a supersonic diffuser.

Couette Flow

The physical domain consisted of stationary lower wall at $j = 1$, uniformly moving upper wall at $j = 16$, and two periodic boundaries at $i = 1 + ½$ and $i = 10 + ½$. The computational domain had 16 grid lines in the η direction and 11 grid lines in the ξ direction. Several cases were run for Reynolds numbers based on the distance between the upper and lower wall between 6.2 and 2.3×10^3 at Mach numbers between 0.09 and 0.75. Courant numbers in the η direction of up to 1000 did not cause any problems, but the Courant number in the ξ direction was limited to $\mathcal{O}(1)$ by the periodic boundary conditions. Depending on the Reynolds number and the Courant number, the steady-state solution was reached after 10-500 iterations. The results for $U_{up} = 0.75$ are shown in Fig. 1.

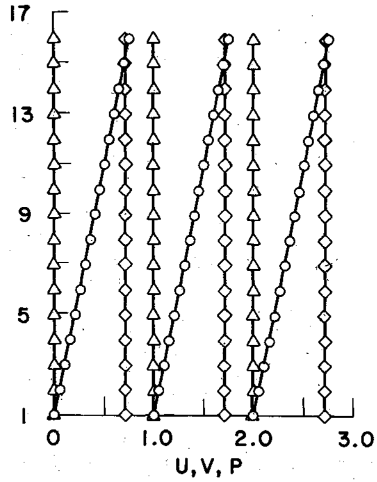

Fig. 1 Velocity and pressure profiles for Couette flow at different streamwise stations.

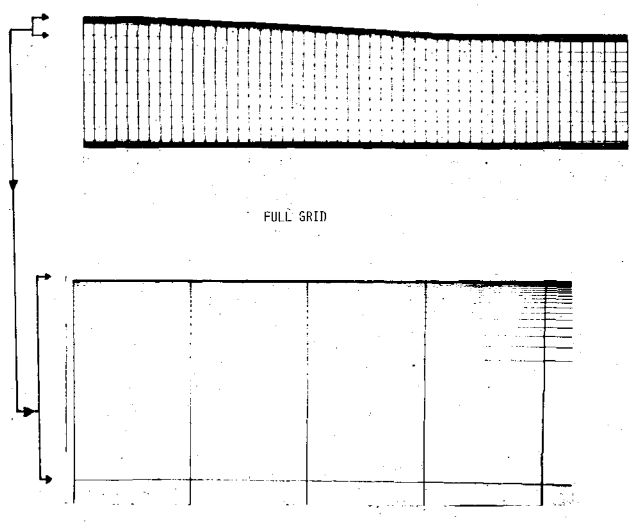

Fig. 2 Supersonic diffuser grid.

Supersonic Diffuser

The supersonic diffuser flow calculation was performed to test the present method on a more demanding case for which analytical and experimental data are available. The diffuser had the shape shown in Fig. 2. It has a straight lower wall and upper wall with a compression corner to produce a shock of required strength. The orthogonal grid shown in Fig. 2 was numerically generated. There were 51 grid lines in the η direction and 51 grid lines in the ξ direction, with 20 grid lines in the viscous layer region close to the wall. Upstream, the Mach number was 2 and the velocity distribution corresponded to $Re_x = 1.25 \times 10^4$. The pressure ratio across the shock was $P_2/P_1 = 1.2$; it was chosen such that direct comparison with experimental results[10] was possible. The boundary layer was assumed to be laminar. At the reflection point the Reynolds number was $Re_x = 3 \times 10^5$. The pressure increase, due to the shock, caused boundary-layer separation. See Fig. 3. The resulting pressure profiles after 600 iterations

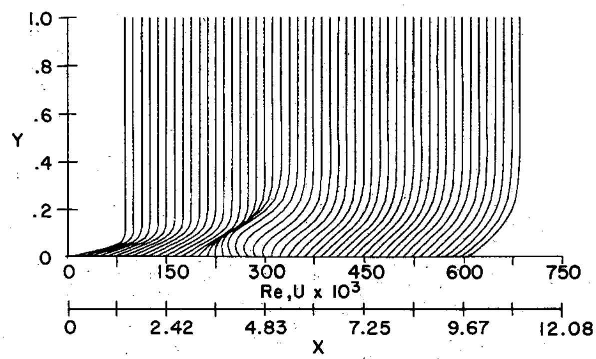

Fig. 3 Boundary-layer velocity profiles computed for lower wall shock/boundary-layer interaction.

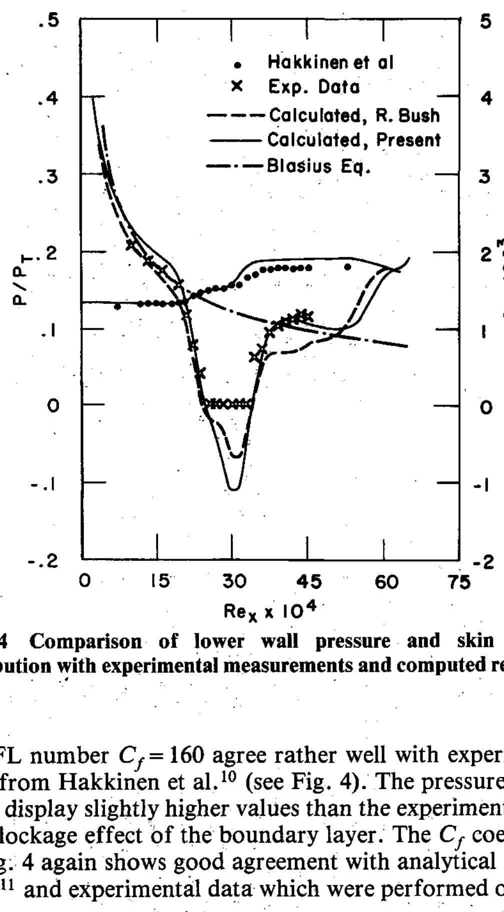

Fig. 4 Comparison of lower wall pressure and skin friction distribution with experimental measurements and computed results.

at CFL number $C_f = 160$ agree rather well with experimental data from Hakkinen et al.[10] (see Fig. 4). The pressures at the walls display slightly higher values than the experiment due to the blockage effect of the boundary layer. The C_f coefficient in Fig. 4 again shows good agreement with analytical data by Bush[11] and experimental data which were performed on a flat plate.

Some problems were experienced with the boundary conditions in the η direction. Best results were obtained by switching sweep directions after one complete time step. The corrector value of δW was reflected off the opposite wall. Although the method has natural dissipation, the steep gradient at the shock/boundary-layer interaction region sometimes caused stability problems. A weak fourth-order explicit damping term was added to the right-hand side term, eliminating the instability.

Conclusion

The present method offers substantial potential for use in complex compressible viscous flow calculations. Using the same Courant numbers, it is faster and simpler than existing implicit methods because it does not require inversion of block tridiagonal matrices. At the present time its use at higher Courant numbers is limited by the choice of boundary conditions to supersonic flows. Its general usefulness for transonic flows depends on future research in the area of boundary conditions.

The implicit part of the boundary conditions deserves special attention as well as the formulation of nonreflective boundary conditions for the inflow and outflow boundaries.

The $\xi = \text{const}$ boundaries (upstream and downstream) did not represent a problem in this case, because the CFL number was here $\sigma(1)$.

Acknowledgments

This research was sponsored by the Office of Naval Research under Contract N00014-81-K-0024, monitored by Dr. Albert Wood.

References

[1] MacCormack, R. W., "The Effect of Viscosity in Hypervelocity Impact Cratering," AIAA Paper 69-354, 1969.

[2] MacCormack, R. W., "Computational Efficiency Achieved by Time Splitting of Finite Difference Operators," AIAA Paper 72-154, 1972.

[3] Beam, R. M. and Warming, R. F., "An Implicit Factored Scheme for the Compressible Navier Stokes Equations," *AIAA Journal*, Vol. 16, April 1978, pp. 393-402.

[4] Pulliam, T. H. and Steger, J. L., "On Implicit Finite Difference Simulations of Three Dimensional Flows," AIAA Paper 78-10, Jan. 1978.

[5] MacCormack, R. W., "A Numerical Method for Solving the Equations of Compressible Viscous Flow," AIAA Paper 81-0110, 1981.

[6] Kumar, A., "Some Observations on a New Numerical Method for Solving the Navier-Stokes Equations," NASA TP 1934, Nov. 1981.

[7] Vinokur, M., "Conservation Equations of Gasdynamics in Curvilinear Coordinate Systems," *Journal of Computational Physics*, Vol. 14, Feb. 1974, pp. 105-125.

[8] Steger, J. L., "Implicit Finite-Difference Simulation of Flow about Arbitrary Two-Dimensional Geometries," *AIAA Journal*, Vol. 16, July 1978, pp. 679-686.

[9] Warming, R. F., Beam, R., and Hyett, B. J., "Diagonalization and Simulations Symmetrization of the Gas-Dynamic Matrices," *Mathematics of Computation*, Vol. 29, Oct. 1975, pp. 1035-1045.

[10] Hakkinen, R. J., Greber, I., Trilling, L. and Abarbanel, S. S., "The Interaction of an Oblique Shock Wave with a Laminar Boundary Layer," NASA Memo 2-18-59W, 1959.

[11] Bush, R. H., "Time Accurate Interval Flow Solutions of the Thin Shear Layer Equations," Gas Turbine and Plasma Dynamics Laboratory, MIT, Rept. 156, Feb. 1981.